




## Article

# A Preliminary Design and Modeling Analysis of Two-Phase Volumetric Expanders for a Novel Reversible Organic Rankine-Based Cycle for Carnot Battery Technology

Sindu Daniarta <sup>1,2,\*</sup> , Piotr Kolasiński <sup>1,\*</sup>  and Attila R. Imre <sup>2,3</sup> 

<sup>1</sup> Department of Thermodynamics and Renewable Energy Sources, Faculty of Mechanical and Power Engineering, Wrocław University of Science and Technology, Wybrzeże Wyspiańskiego 27, 50-370 Wrocław, Poland

<sup>2</sup> Department of Energy Engineering, Faculty of Mechanical Engineering, Budapest University of Technology and Economics, Műegyetem rkp. 3, H-1111 Budapest, Hungary; imreattila@energia.bme.hu

<sup>3</sup> Department of Thermohydraulics, Centre for Energy Research, POB. 49, H-1525 Budapest, Hungary

\* Correspondence: sindu.daniarta@pwr.edu.pl or daniarta@energia.bme.hu (S.D.); piotr.kolasinski@pwr.edu.pl (P.K.)

**Abstract:** Carnot battery technology appears to be a promising solution to increase the development of power generation and offers a good solution for high-capacity, day-to-day energy storage. This technology may utilize the waste heat and store the electricity to recover it later. This article reports the preliminary analysis of a specially designed Carnot battery configuration employing a novel reversible Rankine-based thermodynamic cycle (RRTC). In this case, one volumetric expander is not only installed to generate power from a heat engine, but also to recover power during heat pump operating mode. The preliminary design and modeling results were obtained based on calculations taken from working fluid thermal properties of propane with some specific boundary conditions (i.e., secondary fluid hot temperature of 348.15 K, cooling temperature of 228.15 K, and waste heat temperature of 338.15 K). The results show that isentropic efficiency, pressure, and volumetric expansion ratio from both heat engine and heat pump operating modes are important parameters that must be taken into account when designing the two-phase expander for RRTC. The obtained results show that a designed two-phase volumetric expander in RRTC features a pressure ratio of  $2.55 \pm 1.15$  and a volumetric ratio of  $0.21 \pm 0.105$ , and the Carnot battery may achieve the performance of 0.50–0.98.



**Citation:** Daniarta, S.; Kolasiński, P.; Imre, A.R. A Preliminary Design and Modeling Analysis of Two-Phase Volumetric Expanders for a Novel Reversible Organic Rankine-Based Cycle for Carnot Battery Technology. *Appl. Sci.* **2022**, *12*, 3557. <https://doi.org/10.3390/app12073557>

Academic Editors:

Marco Francesconi and M. Antonelli

**Keywords:** ORC; heat engine; heat pump; phase equilibria; reversible thermodynamic cycle

Received: 7 March 2022

Accepted: 29 March 2022

Published: 31 March 2022

**Publisher's Note:** MDPI stays neutral with regard to jurisdictional claims in published maps and institutional affiliations.



**Copyright:** © 2022 by the authors. Licensee MDPI, Basel, Switzerland. This article is an open access article distributed under the terms and conditions of the Creative Commons Attribution (CC BY) license (<https://creativecommons.org/licenses/by/4.0/>).

## 1. Introduction

In order to ensure sustainable energy generation and easy access to electricity and other forms of energy, there is increased interest in the study and development of power generation systems and devices. Moreover, pro-ecological technology has been driving the research in this area into effective and efficient solutions. Therefore, there is some increased interest in the investigation and development of waste heat recovery technologies [1–3] and the utilization of intermittent and fluctuating heat sources [4]. Recent studies on the utilization of intermittent and fluctuating heat sources involving thermal energy storage (TES) also indicate that thermal energy can be stored and used at any time to produce electricity.

In this case, the Carnot battery offers a good solution that can be implemented to utilize and store the waste heat with the help of a heat engine, a heat pump, and TES [5]. A literature review shows that there are three possible types of Carnot battery technologies. These are methods based on the Lamm–Honigmann process, pumped thermal energy storage (PTES, also known as compressed heat energy storage (CHEST) [6]), and liquefied air energy storage (LAES) [5]. In the Carnot battery, the electric energy is stored as sensible or latent heat (i.e., charging schemes); it can then be recovered using several different

heat engine technologies such as Rankine or Brayton cycles [7]. Due to their advantages, such as flexibility to adapt to different operating conditions and working fluids, easier integration of waste heat, relatively low investment and maintenance cost, and compact modular design, Rankine-based cycles are a promising approach for implementation in Carnot batteries. Therefore, our paper focuses on these cycles.

A significant interest in the research related to Rankine-based cycles is visible in many investigations of the selection of a suitable working fluid [8]. In the classical Rankine cycle, water is applied as the working fluid, whereas the organic Rankine cycle (ORC) uses organic working fluid instead of water in a Rankine-based system. The ORC can utilize various working fluids, and its performance depends on the type of applied working fluid used. These fluids are conventionally classified as wet, dry, or isentropic; alternatively, these working fluids can also be classified by special points, A-C-Z-M-N [9], located on their  $T$ - $s$  diagrams. The ORC system performance depends not only on the applied working fluid but also on the system architecture, which includes simple, cascaded, combined, reheated, and regenerative systems, and those integrated with two-phase expansion cycles [10]. Recent articles [11,12] discussed the maximal efficiency of ORC and its gradual efficiency trendline in a simple design compared with the trilateral flash cycle (TFC) and the partially evaporated ORC (PE-ORC). This simple approach is a benefit for engineers in designing and operating a compact and efficient ORC system. By applying a recuperator, the efficiency of the ORC system in which dry working fluid is applied can be improved [13].

Since the Carnot battery can be implemented using a Rankine-based cycle, various design schemes exist depending on the employed expanders. Compared to turbines, volumetric expanders appear to be more promising for application in Carnot batteries as they can operate with relatively lower noise and vibration and under two-phase conditions (wetness). Therefore, many technical issues can be avoided, such as droplet condensation during expansion (which may lead to serious problems, i.e., blade erosion) [14,15]. A recent preliminary study [16] discussed the possible application of various types of volumetric machines as two-phase expanders, such as the screw, scroll, and multi-vane systems.

In the literature, a study [17] analyzed the Carnot battery with a Rankine-based system in which the heat pump and heat engine were designed as separate devices (that is, the design employed a compressor, a pump, an expander, and a throttle valve). Two further configurations of the Carnot battery use a Rankine-based system employing a reversible scheme and integrated with an electrical heater [5]. The use of a reversible scheme appears to be promising because it reduces the number of components. The literature presents two possible ways to design the reversible scheme. One scheme utilizes the same heat exchangers (as the condenser and evaporator) with a compressor, a pump, a throttling valve, and an expander in a closed-loop system. Another scheme, which reduces the number of components, uses heat exchangers, a pump, a reversible compressor/expander, and a throttling valve. From the literature review, it appears that there is still room for improvement to design a reversible Rankine-based configuration for Carnot battery technology using a two-phase volumetric compressor/expander coupled with a reversible electric motor/generator.

This work reports the preliminary design and modeling of Carnot battery technology with a reversible Rankine-based system, which is the so-called reversible Rankine-based thermodynamic cycle (RRTC). This work aimed to investigate the performance of one volumetric two-phase compressor/expander installed in a special configuration system for both ORC and heat pump modes. This novel approach is presented to provide a possible alternative scheme for a reversible Rankine-based system, and to study the operating conditions of the two-phase volumetric expander. Here, the performance of the volumetric expander refers to the gradual expander power as a function of pressure and the volumetric expansion ratio. Moreover, the trend in Carnot battery performance ( $\zeta$ ) is also discussed. The use of one expander may recover the power during heat pump mode operating mode, and therefore may lead to significantly lower electric consumption.

This paper is structured as follows. The next section introduces the Carnot battery technology in general and its classification. Section 3 reports the novel RRTC system and the mathematical description of the process which was used in the modeling and simulation. Section 4 discusses the results obtained from the modeling of the proposed RRTC system. Finally, the conclusions of the study are summarized.

## 2. Carnot Battery Technology

A Carnot battery is an innovative approach to electrical energy storage (EES) which consists, at least, of electrical input and output [5]. The operating principle of the Carnot battery is simple. The electric energy is first converted to thermal energy, then stored in TES (during TES charging), and can later be recovered (during TES discharging). The charging and discharging can proceed due to several energy conversion technologies. Based on literature studies [5,7], patents related to Carnot battery technology date back to 1979, and the original concept was suggested in 1922 by Marguerre. According to various studies, Carnot batteries may include technology such as pumped thermal electricity storage (PTES) [18], which can be traced back to John Ericsson's work in 1883 [5,19]. A Carnot battery consists of a heat pump, a heat engine, and a high/low-temperature control region during operation, and is illustrated in the literature [5].

In one case, electric energy is used to pump the heat from a low temperature to a high-temperature reservoir, which can be performed with the help of a heat pump. Once the thermal energy is collected in the high-temperature reservoir and TES is charged, thermal energy can be stored for a certain time period. Then, the energy of this high-temperature reservoir can be utilized to generate electricity with the help of heat engines. In another case, the electric input is used to pump the cooled or liquefied working fluid to a low-temperature reservoir (the temperature of which is below the ambient temperature) with the help of a heat pump. This kind of cold energy can then be utilized to generate electricity with the help of a heat engine whose lower operating temperature (i.e., a condenser temperature) is designed around this point. This can even be performed by a cryogenic cycle that works significantly below room temperatures.

There are many possible configurations of Carnot batteries. One example is PTES (which can also be called pumped heat energy storage (PHES) or compressed heat energy storage (CHEST)) [20]. This type of battery may be configured using Rankine-based or Brayton-based cycles with further sub-classes [5].

The Lamm–Honigmann process is a form of thermochemical energy storage invented to be charged with the input of heat or mechanical work, and discharged with the release of heat or mechanical work [21]. The discharging of the Lamm–Honigmann process can be achieved by heating a solution of water in another liquid (e.g., LiBr or NaOH) [5]. In liquefied air energy storage (LAES), electric energy is used to liquefy air with the help of air compression and an air-cooling system (the so-called liquefaction process).

Both Brayton-based and Rankine-based systems show promise for application in Carnot batteries. Brayton-based cycles mainly operate under gas conditions, whereas Rankine-based cycles may involve the two-phase condition. Typical configurations for Brayton- and Rankine-based systems consist of a separated system (heat pump and heat engine), a reversible system (heat pump and heat engine in one compact system), and a combined system with an electrical heater.

The significant difference between Brayton- and Rankine-based cycles is in the energy consumption: the Rankine-based cycle consumes relatively lower power to pump the working fluid than the Brayton cycle [22]. The Rankine cycle features a closed-loop cycle, and the Brayton cycle operates in an open loop. It has been found that the Brayton cycle may work in a closed-loop configuration if it employs a compressor in the process, in which the operating conditions and efficiency may be sensitive to the polytropic performance of the machine [5]. For this reason, in this study, we selected the Rankine-based cycle because it offers good performance and low power consumption of the pump.

There are various potential means to design a reversible heat pump/ORC system; two possibilities are shown in literature. A previous study [23] investigated the RRTC with two heat exchangers (as the reversible condenser and evaporator), a pump, a throttle valve, an expander, and a compressor. Another design of the RRTC [24] was configured to reduce the number of components by employing an expander/compressor device (i.e., a reversible machine). The application of a volumetric machine acting as a compressor/expander in this system may be promising because it can reduce the investment cost of the installation. However, since an expansion process is necessary for both cycles (heat pump and ORC), a study [25] discussed the potential replacement of the throttle valve with an axial piston expander to reduce power consumption. Due to this solution, the coefficient of performance (COP) of the heat pump may be improved. Since the idea of using an expander instead of a throttle valve is promising, in the current paper, the use of a two-phase volumetric expander in the RRTC is discussed in detail in Section 3.

### 3. A Novel Model of the Reversible Rankine-Based Thermodynamic Cycle (RRTC)

#### 3.1. A Proposed Design of the Reversible Rankine-Based Thermodynamic Cycle (RRTC)

The Organic Rankine cycle (ORC) is a Rankine cycle utilizing an organic working fluid instead of water, whereas the heat pump cycle (refrigerating cycle) is a reversed Rankine cycle. The main operating purpose of the ORC is to generate electricity, whereas the main operating purpose of the heat pump is to heat (or cool) the enclosed space.

The thermodynamic processes of these cycles are different. However, it was found that, taking into account the design, these cycles have very similar components, such as heat exchangers (one heat absorber and one cooler), a machine to transfer and pressurize the working fluid (a pump in the ORC and a compressor in the heat pump), and an expander. The literature review showed that the ORC system [8,10] or heat pump [25,26] is usually designed as a stand-alone unit for a single application (generating power or heating/cooling).

Continental climate and seasonal temperature fluctuations are characteristic of many areas globally. In these areas, the application of the ORC and heat pumps is especially interesting. However, the applied designs of these systems, as described above, may lead to significant investment costs due to the necessity of installing two separate units. As an alternative, a promising and novel reversible Rankine-based thermodynamic cycle (RRTC), comprising a heat pump and the ORC, is proposed. The proposed design of this system and its thermodynamic processes are illustrated in the  $T$ - $s$  diagram in Figure 1. It should be noted that, in Figure 1, the maximal and minimal cycle temperatures for both cycles are not the same because the heat pump utilizes waste heat during the operation. In this case, if there are no waste heat recovery/sufficient heat sources, the maximal and minimal cycle temperatures for both cycles may be in the same range. HE1 and HE2 represent heat exchanger 1 (as the heat absorber for the ORC and the heat sink for the heat pump) and heat exchanger 2 (as the heat absorber for the heat pump and the heat sink for the ORC). EXR, CPR, and LP are expander, compressor, and liquid pump, respectively. Moreover, CV and GM are control valves and the reversible generator-motor. In terms of practical aspects, installing a reversible generator-motor may entail several considerations, such as shaft layout and regulation of the shaft when the pump or compressor is not in use. This configuration will also have a significant impact on the efficiency of the generator (which generates the electricity) or the motor (which drives the pump/compressor). To improve the efficiency of a reversible motor-generator, several different factors must be considered. As a result, future experimental study of reversible motor-generators will be interesting.

Counter-flow heat exchangers, as illustrated in Figure 1 for both HE1 and HE2, and indicated by the direction of the input/output and the working fluid inside the cycle, are used to create a more efficient system. Since the heat exchangers in this system are designed in a fixed geometry, and these devices behave as both condenser and evaporator for ORC and heat pump modes (and vice versa), regulating the mass flow rate to match the energy balance occurring in this heat transfer is a possible practical aspect of this design.

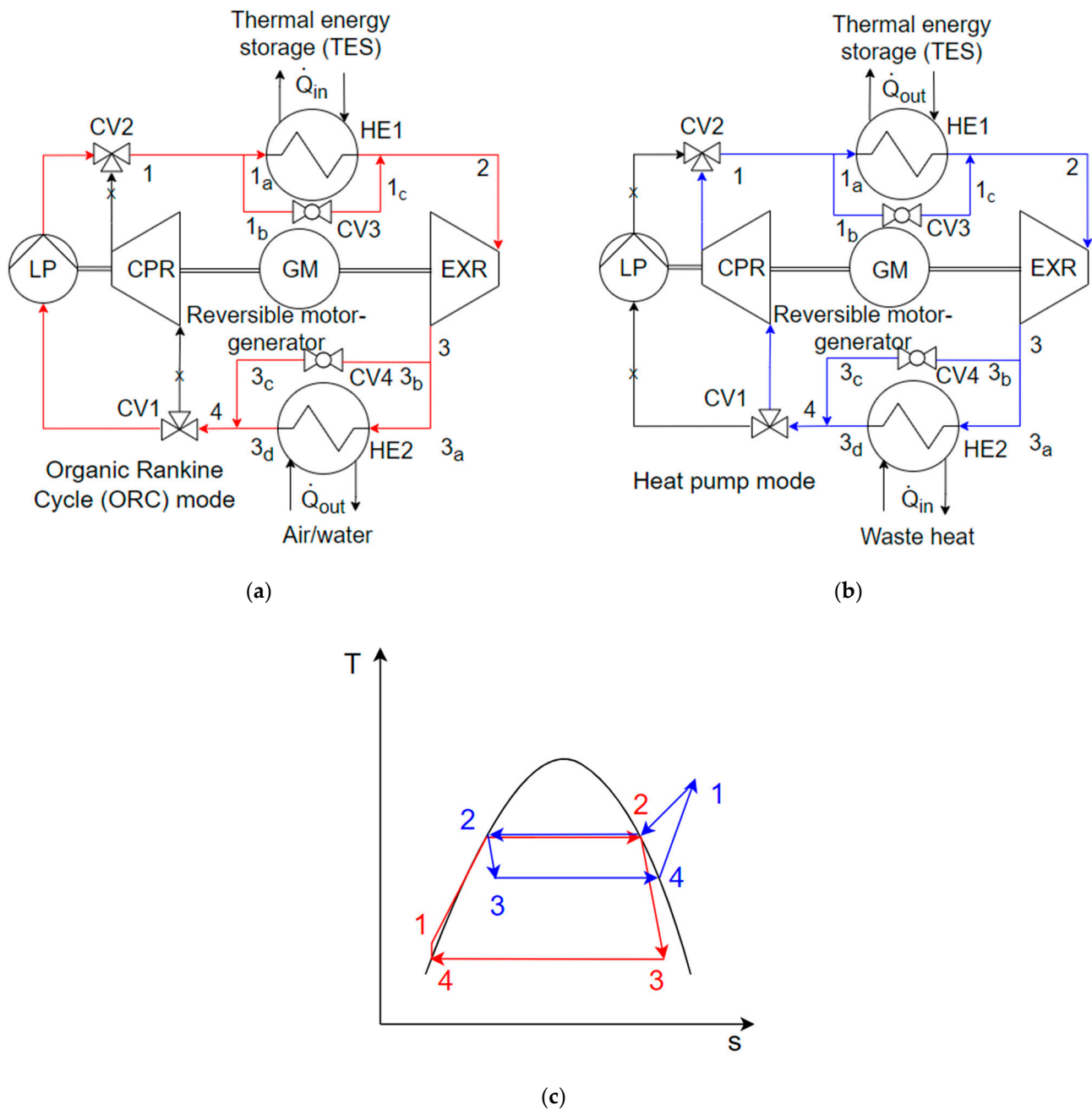


**Figure 1.** The proposed design of a novel reversible Rankine-based thermodynamic cycle (RRTC): the operating scheme for (a) the organic Rankine cycle (ORC), (b) the heat pump, and (c) its processes in a  $T$ - $s$  diagram with the same temperature range (blue lines represent heat pump mode and red lines represent ORC mode, referring to the stream of working fluid through each component).

Figure 1 shows a system that may be utilized for two different tasks (i.e., a switch-like system). This system may be appropriate for continental climate areas and those with limited heat sources that may require cooling at a specific period (i.e., not continuously). The implementation of this RRTC may be beneficial since it is more cost effective than installing two separate devices. In the RRTC, some investments, such as pipelines, heat exchangers, and other components may be reduced. This is the main advantage and innovation of the proposed system.

Figure 1 illustrates that the RRTC in ORC mode indicates red process lines, whereas heat pump mode refers to blue process lines. The control valve must be installed as a



regulator to switch between the processes from ORC to heat pump modes. These regulators have to be placed at the inlet and outlet of the pump or compressor, which increase the pressure of the working fluid in the liquid phase (for the ORC), and the superheated gas or two-phase ( $0 < x < 1$ ) mixture (for the heat pump). Figure 1 illustrates that the liquid pump and compressor act to increase the pressure for ORC and heat pump modes. In this case, the pump is operating for the liquid phase while the compressor is operating for the vapor phase of the working fluids.

In addition to a machine to transfer and pressurize the inlet and outlet working fluid, regulators must also be applied for the heat exchangers because the RRTC requires a single apparatus (see the heat exchanger side for the RRTC illustrated in Figure 1a,b). This regulator helps to regulate the working fluid flow rate through the heat exchanger; therefore, it can successfully change the phase of working fluids.

Environmental impacts are often assessed based on ozone depletion potential (ODP) and global warming potential (GWP), and require that suitable and pro-ecological working fluids are used in further applications. Moreover, some working fluids have been phased out or are forbidden by the Montreal and Kyoto Protocols, or the Kigali Amendment [27]. Therefore, the use of a natural working fluid, which has a relatively low impact on the environment, seems to be promising. Propane is a natural working fluid that appears to be a good candidate because it has low toxicity, zero ODP, and relatively low GWP, and is environmentally friendly. Therefore, this study used propane as the working fluid for the RRTC. The thermal properties and other parameters of propane are listed in Table 1.

**Table 1.** Thermal properties and other parameters of propane [28,29].

Parameters	Value
Name	Propane
CAS number	74-98-6
Formula	C <sub>3</sub> H <sub>8</sub>
R name	R-290
Working fluid type [9]	ACZ (or wet working fluid)
Molar mass (g/mol)	44.09562
ODP	0
GWP	3.3
Safety based on ASHRAE designation	A3
Critical temperature (K)	369.89
Critical pressure (MPa)	4.2512
Critical density (mol/dm <sup>3</sup> )	5
Triple point temperature (K)	85.525
Normal boiling temperature (K)	231.036

A literature review shows that propane has been investigated as a suitable candidate as a working fluid [30] and applied to the ORC [31,32], cascaded cycle [33], and transcritical cycle [34]. It is also used for the Joule–Thompson refrigeration cycle [35] and air conditioning/refrigeration [36,37]. Moreover, because propane is a well-known and widely used substance, the development of novel parts (such as lubricant, etc.) may be unnecessary. Because it is an A3 working fluid, the hermetic seal needs to be considered.

In modeling, the process can be calculated using thermophysical properties such as REFPROP [28] and CoolProp [29] using enthalpy changes. The mathematical description for each mode is discussed in the following sections: Section 3.2 for ORC mode and Section 3.3 for heat pump mode.

### 3.2. The Mathematical Description of RRTC in ORC Mode

In the ORC mode of the RRTC, the heat carrier enters the HE1 with a certain mass flow rate through the pipelines. The energy balance in this device between the heat source and the working fluid inside the cycle can be described by Equations (1)–(3), as follows:

$$\dot{Q}_{in} = \dot{Q}_{HE1}, \quad (1)$$

$$\dot{Q}_{HE1} = \dot{m}_{wf} \Delta h_{1 \rightarrow 2}, \quad (2)$$

$$\dot{m}_{in} \Delta h_{in} = \dot{m}_{wf} \left( \left( c_{p,wf} \Big|_1^{T_{sat,l}} \Delta T_{1 \rightarrow sat,l} \right) + \Delta h_{sat,l \rightarrow 2} \right), \quad (3)$$

where  $\dot{Q}$ ,  $\dot{m}$ , and  $\Delta h$  describe the heat transfer rate, working fluid mass flow rate, and working fluid specific enthalpy changes, respectively. Subscripts wf, in, sat, and l represent working fluid, input (heat carrier), saturation, and liquid, respectively. In addition, other subscripts indicated in Equations (1) and (2) relate to the process in Figure 1a,c. In this case, the energy balance of the heat source and working fluid inside the cycle may be calculated as a function of enthalpy or temperature changes.

In the following step, the expansion process starts when the working fluid reaches the saturated vapor state ( $x = 1$ ), which is indicated with the number 2 (red color) in Figure 1. The real expansion process in the expander can be expressed as a function of enthalpy change by introducing the expander's isentropic efficiency, described by Equations (4) and (5):

$$P_{EXR} = \dot{m}_{wf} \Delta h_{2 \rightarrow 3is} \eta_{EXR,is}, \quad (4)$$

$$\eta_{EXR,is} = \frac{\Delta h_{2 \rightarrow 3}}{\Delta h_{2 \rightarrow 3is}}, \quad (5)$$

where  $P$  and  $\eta$  represent the power and the efficiency, respectively. The subscript "is" represents the isentropic process. The following process is the working fluid condensation (using HE2, illustrated in Figure 1a,c) to alter the phase of working fluid back into a liquid state ( $x = 0$ ). Then, liquified working fluid is ready to be pumped (using LP, presented in Figure 1a,c), and the cycle completes. The process in the condenser (HE2) and pump (LP) can also be expressed using a function of enthalpy changes, described by Equations (6)–(8) for the condenser and Equations (9) and (10) for the pump:

$$\dot{Q}_{out} = \dot{Q}_{HE2}, \quad (6)$$

$$\dot{Q}_{HE2} = \dot{m}_{wf} \Delta h_{3 \rightarrow 4}, \quad (7)$$

$$\dot{m}_{out} \Delta h_{out} = \dot{m}_{wf} \Delta h_{3 \rightarrow 4}, \quad (8)$$

$$P_{LP} = \dot{m}_{wf} \Delta h_{4 \rightarrow 1is} / \eta_{LP,is}, \quad (9)$$

$$\eta_{LP,is} = \frac{\Delta h_{4 \rightarrow 1is}}{\Delta h_{4 \rightarrow 1}}. \quad (10)$$

Using the Equations (1), (4), and (9), the overall efficiency of the RRTC in ORC mode can be expressed as Equation (11):

$$\eta_{RRTC,ORC} = \frac{P_{EXR} - P_{LP}}{\dot{Q}_{HE1}}. \quad (11)$$

### 3.3. The Mathematical Description of RRTC in Heat Pump Mode

The process of the RRTC in heat pump mode starts at HE1, whose power is directly related to the heat transfer rate needed to heat/cool the space. In the mathematical description, it can be calculated as an expression of enthalpy changes, in the same way as in Equation (2) according to energy balance. However, it has to be noted that the process

operates in the opposite direction. This means that using the same heat exchanger, in heat pump mode, the HE1 behaves as a condenser instead of an evaporator. Therefore, a special design of HE1 has to be implemented. The condensation process in HE1 starts from the superheated state and proceeds to the liquid state ( $x = 0$ ), which is referred to the states numbered 1 and 2 (blue color) in Figure 1b,c. Therefore, the process of HE1 in heat pump mode can be expressed as a function of enthalpy changes, described as Equation (12):

$$\dot{m}_{\text{out}}\Delta h_{\text{out}} = \dot{m}_{\text{wf}} \left( (c_{p,\text{wf}} \Big|_{T_2}^{T_{\text{sat},v}} \Delta T_{2 \rightarrow \text{sat},v}) + \Delta h_{\text{sat},v \rightarrow 1} \right), \quad (12)$$

where the subscript v represents the vapor.

Once the working fluid reaches a saturated liquid state ( $x = 0$ ), which is indicated by state 2 (blue color) in Figure 1b,c, the working fluid needs to be expanded. In small heat pumps, the throttle valves were often used as the expansion devices. Because this novel RRTC uses an innovative expansion device, the expander is used to expand the working fluid; therefore, no throttle valve is installed. It should be noted that the use of expansion devices for expanding saturated liquids is a realistic assumption; similar devices are used in flash cycles [38]. The expansion process of the RRTC in heat pump mode can be described as in Equations (4) and (5).

The following process is the evaporation during which the working fluid changes the phase from two-phase ( $0 < x < 1$ ) to saturated vapor ( $x = 1$ ) or superheated state, as presented in Figure 1b,c, indicated with the state 3 and 4 (blue color). Although the same heat exchanger (HE2) can be utilized in the RRTC operating in heat pump mode, the process has a different direction, as shown in Figure 1b,c. The evaporation process in HE2 can be expressed as Equation (7) for the enthalpy change. Therefore, the process of HE2 in heat pump mode can be described as Equation (13):

$$\dot{m}_{\text{in}}\Delta h_{\text{in}} = \dot{m}_{\text{wf}}\Delta h_{3 \rightarrow 4}. \quad (13)$$

The possible application of plate heat exchangers as a reversible device (condenser and evaporator) has been discussed elsewhere [39]. After the previous step, the working fluid is ready to be pressurized with the help of a compressor. Typically, the compressor process is similar to using a pump to increase the working fluid's pressure, but in the vapor/gas phase. The compressor power and isentropic efficiency can be expressed using the change in the specific enthalpy of the working fluid, as described in Equations (14) and (15):

$$P_{\text{CPR}} = \dot{m}_{\text{wf}}\Delta h_{4 \rightarrow 1_{\text{is}}} / \eta_{\text{CPR, is}}, \quad (14)$$

$$\eta_{\text{CPR, is}} = \frac{\Delta h_{4 \rightarrow 1_{\text{is}}}}{\Delta h_{4 \rightarrow 1}}. \quad (15)$$

Therefore, the coefficient of performance of the RRTC operating in heat pump mode can be expressed as Equation (16):

$$COP_{\text{RRTC, heat pump}} = \frac{P_{\text{CPR}} - P_{\text{EXR}}}{\dot{Q}_{\text{HE1}}}. \quad (16)$$

### 3.4. System Setup

The main advantage of the proposed novel RRTC is that the system uses the same heat exchangers (HE1, HE2) and expander (EXR) (as illustrated in Figure 1) in both ORC and heat pump operating modes. In this study, it was assumed that the heat exchangers are isobaric. The system setup of this study is shown in Table 2. The system model was implemented and computed using MATLAB, and the thermal properties of the working fluid were taken from CoolProp [29].



**Table 2.** The reversible Rankine-based thermodynamic cycle (RRTC) setup applied in this study.

Parameters	ORC Mode	Heat Pump Mode
HE1 pinch point (K)	5	5
HE2 pinch point (K)	5	5
HE1 secondary fluid temperature (K)	348.15—348.15 + 10 (from storage)	348.15—348.15 + 10 (to storage)
HE2 secondary fluid temperature (K)	288.15 (from air)	338.15 (from waste heat)
Simulation temperature step (K)	1	1
Isentropic efficiency of expander (-)	0.8 and 0.7	$\eta_{\text{EXR, is}} < 0.8$
Isentropic efficiency of a pressure riser device (-)	0.8 (a liquid pump)	0.8 (a compressor)

The secondary fluid temperature was set starting from 348.15 K, and the air and waste heat temperatures were set to 288.15 and 338 K, respectively, to study the feasible performance of the power generation below 373.15 K. In several countries (for example in Hungary and Poland), central heating for blockhouses uses hot water having a temperature of 60–70 °C [40]. In addition, these conditions are typical for many industrial applications, and they should result in an electrical output that is equal to the electrical consumption [41]. In modeling, it was assumed that the efficiency of TES is equal to 1, and the mass flow rate of the working fluid is equal to 1 kg/s. Therefore, the performance of the Carnot battery unit can be determined by the multiplication of *COP* and ORC efficiency, which is described as Equation (17) [42]:

$$\zeta = \frac{COP_{\text{RRTC, heat pump}}}{\dot{Q}_{\text{HE1, heat pump}}} \eta_{\text{RRTC, ORC}} \dot{Q}_{\text{HE1, ORC}} = COP_{\text{RRTC, heat pump}} \eta_{\text{RRTC, ORC}} \quad (17)$$

#### 4. Results and Discussion

Different types of volumetric expanders can be potentially applied in the considered system, such as gerotor, scroll, screw, piston, and multi-vane expanders [43,44]. Each type of expander has its own operating characteristics, geometry, and design [45,46]. A previous study [16] examined and discussed the possibility of applying volumetric expanders in different operating conditions, including two-phase expansion. This investigation shows that, compared to reciprocating volumetric expanders (i.e., piston expanders), some rotary volumetric expanders (e.g., multi-vane machines) tend to work under two-phase conditions without any serious issues. Therefore, the rotary type of two-phase volumetric expanders may be suitable for application in a reversible Rankine-based Carnot battery.

When designing the volumetric expanders, two important parameters, namely, pressure and volumetric expansion ratio, must be considered. These parameters can be expressed as described in Equations (18) and (19):

$$\delta_p = \frac{p_{\text{in}}}{p_{\text{out}}} = \frac{p_2}{p_3} \quad (18)$$

$$\delta_V = \frac{\dot{V}_{\text{in}}}{\dot{V}_{\text{out}}} = \frac{\dot{m}_{\text{in}}/\rho_{\text{in}}}{\dot{m}_{\text{out}}/\rho_{\text{out}}} = \frac{\rho_{\text{out}}}{\rho_{\text{in}}} = \frac{\rho_3}{\rho_2} \quad (19)$$

where subscripts *p* and *V* represent the pressure and volume, respectively. Moreover, *p*,  $\dot{V}$ , and  $\rho$  describe pressure, volumetric flow rate, and density, respectively.

The MATLAB configuration model was validated using experimental data from a previous study [47] using a multi-vane expander, and both modeling and experimental results are plotted in Figure 2. The validated results show that the MATLAB configuration model has a 1–3% relative error. Some parameters, such as heat losses, internal friction, and other characteristics that were not considered in the modeling, may result in inaccuracy. In this case, only isentropic expander efficiency was established in the configured model.

Using the data from the MATLAB model appears to be a good approach for obtaining the expected result during the design stage because the relative error was observed to be less than 10%.

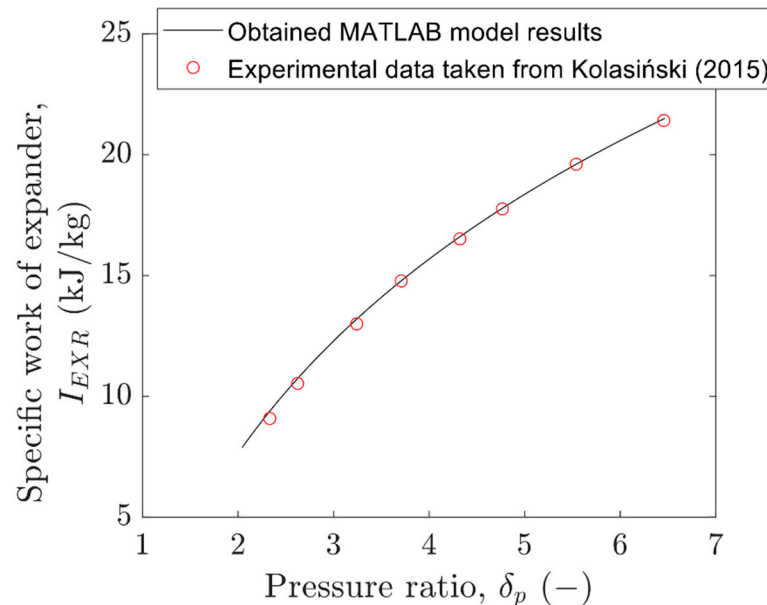


**Figure 2.** The obtained data from the MATLAB configuration validated using the experimental data from prior work.

The following section presents and discusses the modeling data based on the working fluid thermal properties concerning the power of the expander if it runs in both modes (i.e., heat pump and ORC modes). The obtained modeling results shown in pressure ratio–power and volumetric ratio–power diagrams are presented in Figure 3. This figure shows that, with the assumption of a mass flow rate at 1 kg/s for both operating modes, the generated power varies as a function of pressure and volumetric expansion ratios.

Figure 3 illustrates the variation in the two-phase volumetric expander power operating in ORC and heat pump modes. The output power of this expander for ORC mode is around 23–43 kW, whereas for heat pump mode it is around 1.4–5.5 kW. The result shows a big difference between the obtained expander output power for ORC and heat pump modes. In heat pump mode, the expander generates less power than in ORC mode. This is because the change in the specific enthalpy of the working fluid is a function of the temperature range, which, for the heat pump and the ORC, is also different. One significant problem that has to be considered when designing this volumetric expander for the ORC and the heat pump in the RRTC is that the volumetric machine needs to cover the operating pressure ratio of the system working in heat pump and ORC modes. As illustrated in Figure 3a, assuming that the mass flow rate of the working fluids equals 1 kg/s, the resulting pressure expansion ratio in heat pump mode is almost one-third that in ORC mode (the pressure ratio in heat pump mode ranges between 1.47 and 1.77, whereas in ORC mode it ranges between 3.09 and 3.70).

In addition, the applied volumetric expander needs to be fitted into the range of the volumetric ratio based on the obtained results, which are illustrated in Figure 3b. The results show that the range of the volumetric expansion ratio for ORC mode is lower than that for heat pump mode. The volumetric expansion ratio for ORC mode varies in a range of 0.011–0.015, whereas that for heat pump mode varies in a range of 0.33–0.41. Therefore, pressure and volumetric expansion ratio coverage need to be carefully considered in selecting suitable two-phase rotary volumetric expanders.

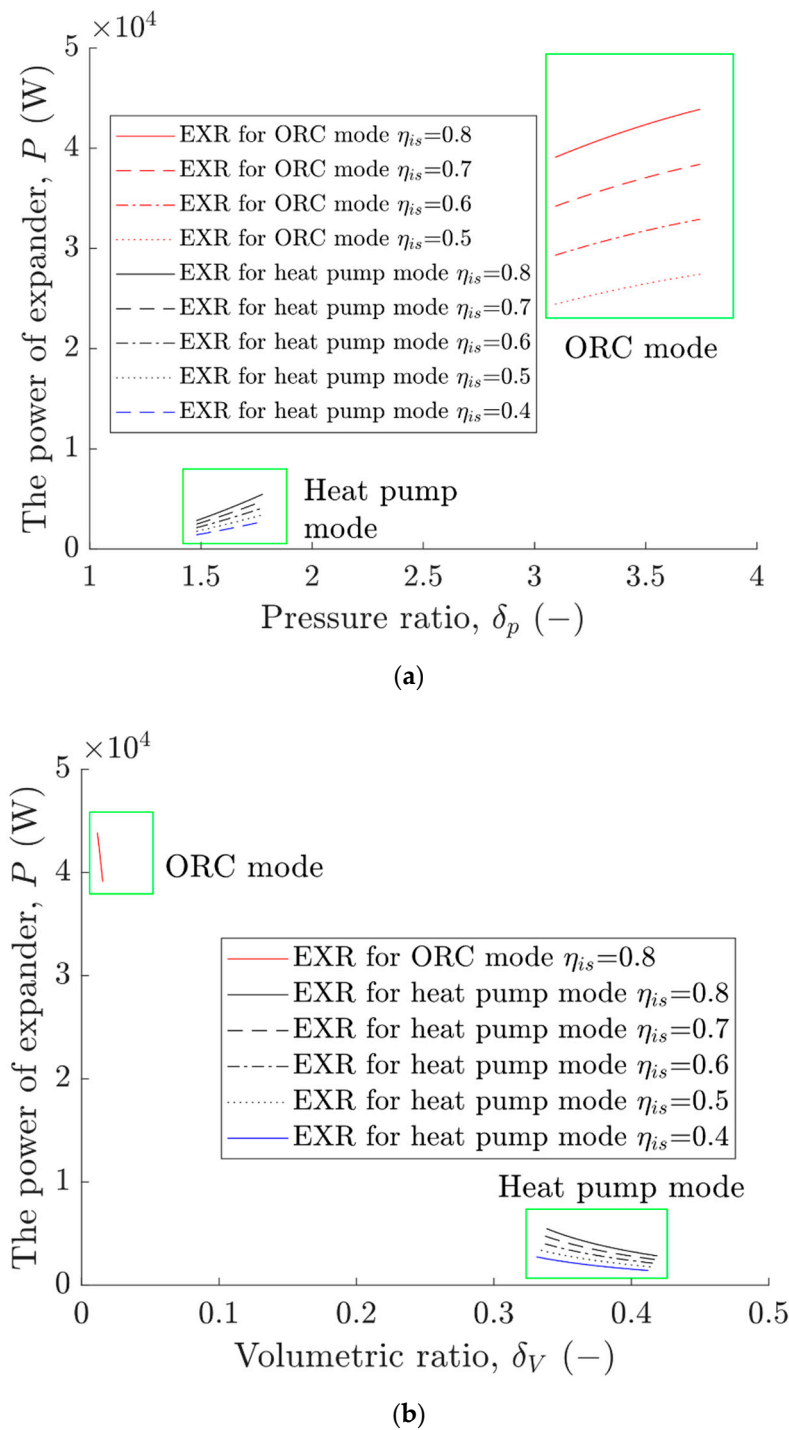


**Figure 3.** The obtained power of the two-phase expander applied in the RRTC in ORC and heat pump modes in (a) pressure ratio–expander power diagram and (b) volume ratio–expander power diagram. Because the throttle valve is replaced by a volumetric expander in the RRTC heat pump, the power of the expander can be calculated not only for the ORC mode, but also for the heat pump mode.

As illustrated in Figure 3, the obtained results were modeled in different isentropic efficiency conditions. A prior study [48] discussed the empirical method based on Baumann’s rule, which bounds the isentropic efficiency of the expander and vapor quality, and is defined as Equation (20):

$$\eta_{EXR, is, wet} = \eta_{EXR, is, dry}(1 - \beta_B(1 - x)), \tag{20}$$

where  $\beta$  is the Baumann coefficient. This empirical method shows that the expander's isentropic efficiency will gradually decrease. Therefore, as illustrated in Figure 1c, the expansion process in heat pump mode may start at the lowest vapor quality near the saturated liquid state ( $0 < x < 0.2$ ). This is the so-called flashing process. The flashing here occurs in the two-phase region, which can be visualized in the  $T$ - $s$  diagram, referring to Figure 1c for the process 2–3 (blue lines).

The design of the two-phase volumetric expander may be conducted based on the features of the volumetric machine operating in ORC mode, in which the higher isentropic efficiency of the expander needs to be achieved. In this case, the isentropic efficiency of the expander in heat pump mode will follow. However, it is necessary to predict this efficiency and design the system so that the good  $COP$  can be achieved.

The  $COP$  and ORC efficiency are important assessment parameters that have to be considered in this Carnot battery technology; therefore, the values of these parameters were modeled in the present study. The obtained results are plotted in Figure 4, in a  $COP$ –ORC efficiency diagram. The results show that increasing the ORC efficiency will decrease  $COP$  based on the designed RRTC, as illustrated in Figure 1. Figure 4a,b visualizes the results based on the change in expander isentropic efficiency. As discussed above, the design of the expander may be based on the ORC mode. From Figure 4, it can be seen that changing the isentropic efficiency of the expander for ORC mode significantly influences the overall ORC efficiency. It shows that, with an expander isentropic efficiency of 0.8, the overall ORC efficiency ranges between 0.09 and 0.10, whereas, for an expander isentropic efficiency of 0.7, the ORC efficiency drops to 0.08. The obtained values are in good agreement with the research results that were obtained experimentally and numerically by the authors in their earlier studies related to ORC systems equipped with a volumetric expander [49,50].

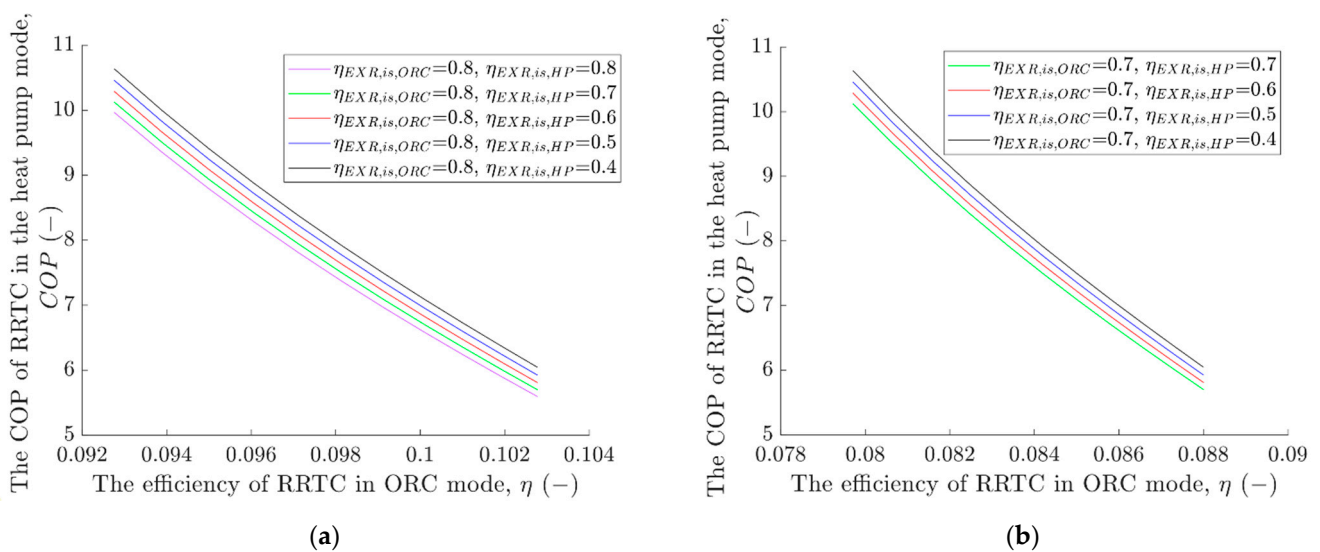


**Figure 4.** The obtained results for the RRTC in  $COP$ – $\eta$  diagrams with the basis efficiency of the expander: (a) 0.8 and (b) 0.7.

In the Carnot battery technologies, the performance can be expressed using Equation (13); therefore, in this discussion, the obtained results of this parameter ( $\zeta$ ) are also presented here, as illustrated in Figure 5. The obtained results show the comparison between  $\zeta$  with an isentropic efficiency of the expander in ORC and heat pump modes. The results show that  $\zeta$  can be expressed as a function of HE1 temperature, and the conclusion can be drawn that increasing HE1 temperature decreases  $\zeta$ .

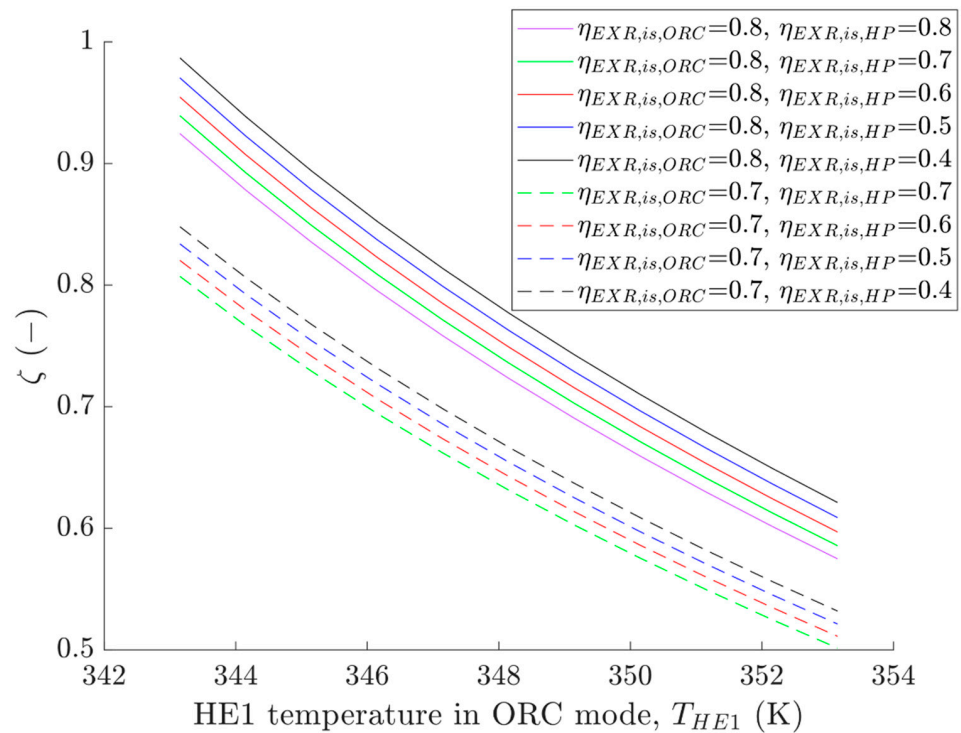


**Figure 5.** The variation in  $\zeta$  for different values of  $T_{HE1}$  temperature and different expander isentropic efficiency.

Figure 5 shows that the expander's isentropic efficiency significantly influences the Carnot battery's performance. The obtained result shows that, when the isentropic efficiency of the expander is equal to 0.8, the  $\zeta$  parameter of the RRTC ranges between 0.6 and 0.98; and when the isentropic efficiency of the expander is equal to 0.7, the  $\zeta$  parameter is in the range of 0.53–0.84 (which is about 14% lower). It appears that, if the isentropic efficiency of the expander operating in ORC mode is equal to 0.8, and assuming that the isentropic efficiency of the expander operating in heat pump mode is 0.5, it can be concluded that the  $\zeta$  parameter is still relatively higher than the isentropic efficiency of the expander for both ORC and heat pump modes. In this case, the difference is about 9.79%.

The above-mentioned novel RRTC design using one expander for ORC and heat pump modes may be an alternate solution for a more cost-effective Carnot battery design. In this case, further study and analysis considering some important aspects (such as the thermo-economics, technical issues relating to the type and design of suitable expanders, structural analysis, wear, lubricants, bubble growth, and working fluids) would be interesting to discuss in the future.

## 5. Conclusions

This paper discusses the result of a modeling analysis of the possible application of two-phase volumetric expanders for a novel reversible Rankine-based cycle for Carnot batteries. The results of this study show a significant difference in the values of the assessment parameters, such as pressure ratio, volumetric expansion ratio, and output power for the same volumetric expander working in ORC and heat pump modes. These parameters have to be considered together during the design and selection of two-phase volumetric expanders that can operate in both ORC and heat pump modes. To implement a single expander to generate power from ORC mode and reduce the power consumption of heat pump mode (by installing an expander instead of a throttle valve), it is suggested to design the expander based on the values of the assessment parameters obtained for ORC mode, and then fit the design in a way that covers the pressure and volumetric expansion ratio needed for the system operation in heat pump mode.



The obtained result of the RRTC modeling simulation using propane as the working fluid shown in the power–pressure ratio diagram illustrated in Figure 3a shows that, if one expander is applied for both cycles (ORC and heat pump modes), this expander needs to cover the pressure ratio between 1.4 (minimal) and 3.7 (maximal). In addition, this device is also required to cover the volumetric ratio between 0.01 (minimal) and 0.41 (maximal), as depicted in the power–volumetric ratio diagram (Figure 3b). Therefore, it is suggested to design the expander in the RRTC mentioned above having a pressure ratio of  $2.55 \pm 1.15$  and a volumetric ratio of  $0.21 \pm 0.105$ . It may be possible to obtain these design parameters if rotary-type volumetric machines, such as multi-vane expanders, are applied in the RRTC system. Using these parameters, performance of Carnot battery technology in the range of 0.50–0.98 may be achieved with an HE1 temperature in ORC mode of 343.15–353.15 K.

**Author Contributions:** Conceptualization, methodology, software, validation, formal analysis, investigation, visualization, writing—original draft preparation, S.D.; writing—review and editing, S.D., P.K., A.R.I.; supervision, P.K., A.R.I.; All authors have read and agreed to the published version of the manuscript.

**Funding:** This work was supported by NAWA STER Program Internationalization of Wrocław University of Science and Technology Doctoral School.

**Institutional Review Board Statement:** Not applicable.

**Informed Consent Statement:** Not applicable.

**Data Availability Statement:** Not applicable.

**Acknowledgments:** The authors would like to thank Marco Antonelli and Marco Francesconi for the invitation to publish this article.

**Conflicts of Interest:** The authors declare no conflict of interest.

## Nomenclature

$c$	The specific heat capacity (J/kg·K)
$h$	The specific enthalpy (J/kg)
$I$	The specific work of expander (kJ/kg)
$\dot{m}$	Mass flow rate (kg/s)
$P$	Power (Watt)
$P$	Pressure (Pa)
$T$	Temperature (K)
$\dot{Q}$	Heat transfer rate (Watt)
$\dot{V}$	Volumetric flow rate (m <sup>3</sup> /s)
$x$	Vapor quality (–)

Greek letters:

$\beta$	Baumann coefficient
$\delta$	Ratio (–)
$\eta$	Efficiency (–)
$\zeta$	Performance of Carnot battery (–)
$\rho$	Density (kg/m <sup>3</sup> )

Subscripts:

1,2,3,4	Process in the cycle (blue color for heat pump mode, red color for ORC mode)
B	Baumann rule
CPR	Compressor
EXR	Expander
GM	Reversible motor-generator
HE	Heat exchanger
in	Input
is	Isentropic process
l	Liquid
LP	Liquid pump
out	Output

p	Pressure
sat	Saturation
v	Vapor
V	Volumetric
WF	Working fluids
Abbreviations:	
CHEST	Compressed heat energy storage
COP	Coefficient of performance
CV	Control valve
EES	Electrical energy storage
LAES	Liquefied air energy storage
GWP	Global warming potential
ODP	Ozone depletion potential
ORC	Organic Rankine cycle
PHES	Pumped heat energy storage
PTES	Pumped thermal electricity storage
RRTC	Reversible Rankine-based thermodynamic cycle
TES	Thermal energy storage

## References

- Omar, A.; Saghafifar, M.; Mohammadi, K.; Alashkar, A.; Gadalla, M. A review of unconventional bottoming cycles for waste heat recovery: Part II—Applications. *Energy Convers. Manag.* **2019**, *180*, 559–583. [\[CrossRef\]](#)
- Zhang, X.; Cao, M.; Yang, X.; Guo, H.; Wang, J. Economic Analysis of Organic Rankine Cycle Using R123 and R245fa as Working Fluids and a Demonstration Project Report. *Appl. Sci.* **2019**, *9*, 288. [\[CrossRef\]](#)
- Moradi, R.; Habib, E.; Bocci, E.; Cioccolanti, L. Component-Oriented Modeling of a Micro-Scale Organic Rankine Cycle System for Waste Heat Recovery Applications. *Appl. Sci.* **2021**, *11*, 1984. [\[CrossRef\]](#)
- Li, X.; Xu, B.; Tian, H.; Shu, G. Towards a novel holistic design of organic Rankine cycle (ORC) systems operating under heat source fluctuations and intermittency. *Renew. Sustain. Energy Rev.* **2021**, *147*, 111207. [\[CrossRef\]](#)
- Dumont, O.; Frate, G.F.; Pillai, A.; Lecompte, S.; De Paepe, M.; Lemort, V. Carnot battery technology: A state-of-the-art review. *J. Energy Storage* **2020**, *32*, 101756. [\[CrossRef\]](#)
- Steinmann, W.D. The CHEST (Compressed Heat Energy STORAGE) concept for facility scale thermo mechanical energy storage. *Energy* **2014**, *69*, 543–552. [\[CrossRef\]](#)
- Benato, A.; Stoppato, A. Pumped Thermal Electricity Storage: A technology overview. *Therm. Sci. Eng. Prog.* **2018**, *6*, 301–315. [\[CrossRef\]](#)
- Bao, J.; Zhao, L. A review of working fluid and expander selections for organic Rankine cycle. *Renew. Sustain. Energy Rev.* **2013**, *24*, 325–342. [\[CrossRef\]](#)
- Györke, G.; Deiters, U.K.; Groniewsky, A.; Lassu, I.; Imre, A.R. Novel classification of pure working fluids for Organic Rankine Cycle. *Energy* **2018**, *145*, 288–300. [\[CrossRef\]](#)
- Quoilin, S.; Van Den Broek, M.; Declaye, S.; Dewallef, P.; Lemort, V. Techno-economic survey of Organic Rankine Cycle (ORC) systems. *Renew. Sustain. Energy Rev.* **2013**, *22*, 168–186. [\[CrossRef\]](#)
- Daniarta, S.; Kolasiński, P.; Imre, A.R. Thermodynamic efficiency of trilateral flash cycle, organic Rankine cycle and partially evaporated organic Rankine cycle. *Energy Convers. Manag.* **2021**, *249*, 114731. [\[CrossRef\]](#)
- Ahmed, A.M.; Kondor, L.; Imre, A.R. Thermodynamic Efficiency Maximum of Simple Organic Rankine Cycles. *Energies* **2021**, *14*, 307. [\[CrossRef\]](#)
- Ahmed, A.M.; Imre, A.R. The effect of recuperator on the efficiency of ORC and TFC with very dry working fluid. In *MATEC Web of Conferences*; EDP Sciences: Les Ulis, France, 2021; Volume 345. [\[CrossRef\]](#)
- Dumont, O.; Parthoens, A.; Dickes, R.; Lemort, V. Experimental investigation and optimal performance assessment of four volumetric expanders (scroll, screw, piston and roots) tested in a small-scale organic Rankine cycle system. *Energy* **2018**, *165*, 1119–1127. [\[CrossRef\]](#)
- Smith, I.K.; Stosic, N.; Kovacevic, A. *Power Recovery from Low Cost Two-Phase Expanders*; Transactions of Geothermal Resource Council: Davis, CA, USA, 2001; pp. 601–605.
- Daniarta, S.; Kolasiński, P. A preliminary study of two-phase volumetric expanders and their application in ORC systems. In *Proceedings of the 6th International Seminar on ORC Power Systems, Munich, Germany, 11–13 October 2021*. [\[CrossRef\]](#)
- Frate, G.F.; Ferrari, L.; Desideri, U. Multi-Criteria Economic Analysis of a Pumped Thermal Electricity Storage (PTES) With Thermal Integration. *Front. Energy Res.* **2020**, *8*, 53. [\[CrossRef\]](#)
- Bellos, E.; Lykas, P.; Tzivanidis, C. Pumped Thermal Energy Storage System for Trigeneration: The Concept of Power to XYZ. *Appl. Sci.* **2022**, *12*, 970. [\[CrossRef\]](#)
- Steinmann, W.-D. Thermo-mechanical concepts for bulk energy storage. *Renew. Sustain. Energy Rev.* **2017**, *75*, 205–219. [\[CrossRef\]](#)

20. Steinmann, W.-D.; Bauer, D.; Jockenhöfer, H.; Johnson, M. Pumped thermal energy storage (PTES) as smart sector-coupling technology for heat and electricity. *Energy* **2019**, *183*, 185–190. [[CrossRef](#)]
21. Jahnke, A.; Strenge, L.; Fleßner, C.; Wolf, N.; Jungnickel, T.; Ziegler, F. First cycle simulations of the Honigmann process with LiBr/H<sub>2</sub>O and NaOH/H<sub>2</sub>O as working fluid pairs as a thermochemical energy storage. *Int. J. Low-Carbon Technol.* **2013**, *8*, i55–i61. [[CrossRef](#)]
22. Müller, N.; Frechette, L.G. Performance Analysis of Brayton and Rankine Cycle Microsystems for Portable Power Generation. In Proceedings of the ASME 2002 International Mechanical Engineering Congress and Exposition, Microelectromechanical Systems, New Orleans, LA, USA, 17–22 November 2002. [[CrossRef](#)]
23. Staub, S.; Bazan, P.; Braimakis, K.; Müller, D.; Regensburger, C.; Scharrer, D.; Schmitt, B.; Steger, D.; German, R.; Karellas, S.; et al. Reversible Heat Pump–Organic Rankine Cycle Systems for the Storage of Renewable Electricity. *Energies* **2018**, *11*, 1352. [[CrossRef](#)]
24. Dumont, O.; Carmo, C.; Fontaine, V.; Randaxhe, F.; Quoilin, S.; Lemort, V.; Elmegaard, B.; Nielsen, M.P. Performance of a reversible heat pump/organic Rankine cycle unit coupled with a passive house to get a positive energy building. *J. Build. Perform. Simul.* **2018**, *11*, 19–35. [[CrossRef](#)]
25. Chua, K.J.; Chou, S.K.; Yang, W.M. Advances in heat pump systems: A review. *Appl. Energy* **2010**, *87*, 3611–3624. [[CrossRef](#)]
26. Dai, N.; Xu, X.; Li, S.; Zhang, Z. Simulation of Hybrid Photovoltaic Solar Assisted Loop Heat Pipe/Heat Pump System. *Appl. Sci.* **2017**, *7*, 197. [[CrossRef](#)]
27. Sovacool, B.K.; Griffiths, S.; Kim, J.; Bazilian, M. Climate change and industrial F-gases: A critical and systematic review of developments, sociotechnical systems and policy options for reducing synthetic greenhouse gas emissions. *Renew. Sustain. Energy Rev.* **2021**, *141*, 110759. [[CrossRef](#)]
28. Lemmon, E.; Huber, M.; McLinden, M. *NIST Standard Reference Database 23: Reference Fluid Thermodynamic and Transport Properties-REFPROP, Version 9.1*; National Institute of Standards and Technology: Gaithersburg, MD, USA, 2013.
29. Bell, I.H.; Wronski, J.; Quoilin, S.; Lemort, V. Pure and Pseudo-pure Fluid Thermophysical Property Evaluation and the Open-Source Thermophysical Property Library CoolProp. *Ind. Eng. Chem. Res.* **2014**, *53*, 2498–2508. [[CrossRef](#)] [[PubMed](#)]
30. White, M.T.; Oyewunmi, O.A.; Haslam, A.J.; Markides, C.N. Industrial waste-heat recovery through integrated computer-aided working-fluid and ORC system optimisation using SAFT- $\gamma$  Mie. *Energy Convers. Manag.* **2017**, *150*, 851–869. [[CrossRef](#)]
31. Choi, I.-H.; Lee, S.; Seo, Y.; Chang, D. Analysis and optimization of cascade Rankine cycle for liquefied natural gas cold energy recovery. *Energy* **2013**, *61*, 179–195. [[CrossRef](#)]
32. Gao, W.; Wu, Z.; Tian, Z.; Zhang, Y. Experimental investigation on an R290-based organic Rankine cycle utilizing cold energy of liquid nitrogen. *Appl. Therm. Eng.* **2022**, *202*, 117757. [[CrossRef](#)]
33. Dubberke, F.H.; Linnemann, M.; Abbas, W.K.; Baumhögger, E.; Priebe, K.-P.; Roedder, M.; Neef, M.; Vrabec, J. Experimental setup of a cascaded two-stage organic Rankine cycle. *Appl. Therm. Eng.* **2018**, *131*, 958–964. [[CrossRef](#)]
34. Yu, J.; Xu, Z.; Tian, G. A thermodynamic analysis of a transcritical cycle with refrigerant mixture R32/R290 for a small heat pump water heater. *Energy Build.* **2010**, *42*, 2431–2436. [[CrossRef](#)]
35. Bai, T.; Li, D.; Xie, H.; Yan, G.; Yu, J. Experimental research on a Joule-Thomson refrigeration cycle with mixture R170/R290 for  $-60$  °C low-temperature freezer. *Appl. Therm. Eng.* **2021**, *186*, 116476. [[CrossRef](#)]
36. Yadav, S.; Liu, J.; Kim, S.C. A comprehensive study on 21st-century refrigerants—R290 and R1234yf: A review. *Int. J. Heat Mass Transf.* **2022**, *182*, 121947. [[CrossRef](#)]
37. Ghanbarpour, M.; Mota-Babiloni, A.; Badran, B.E.; Khodabandeh, R. Energy, Exergy, and Environmental (3E) Analysis of Hydrocarbons as Low GWP Alternatives to R134a in Vapor Compression Refrigeration Configurations. *Appl. Sci.* **2021**, *11*, 6226. [[CrossRef](#)]
38. Bianchi, G.; Marchionni, M.; Miller, J.; Tassou, S.A. Modelling and off-design performance optimisation of a trilateral flash cycle system using two-phase twin-screw expanders with variable built-in volume ratio. *Appl. Therm. Eng.* **2020**, *179*, 115671. [[CrossRef](#)]
39. Steger, D.; Regensburger, C.; Pham, J.; Schlücker, E. Heat Exchangers in Carnot Batteries: Condensation and Evaporation in a Reversible Device. *Energies* **2021**, *14*, 5620. [[CrossRef](#)]
40. Pawlik, M.; Strzelczyk, F. *Elektrownie*; Wydawnictwo Naukowe PWN: Warsaw, Poland, 2016; ISBN 978-83-01-18954-9.
41. Dumont, O.; Lemort, V. Modelling of a thermally integrated Carnot battery using a reversible heat pump/organic Rankine cycle. In Proceedings of the ECOS 2020—33rd International Conference on Efficiency, Cost, Optimization, Simulation and Environmental Impact of Energy Systems, Osaka, Japan, 3–29 July 2020.
42. Dumont, O.; Lemort, V. Mapping of performance of pumped thermal energy storage (Carnot battery) using waste heat recovery. *Energy* **2020**, *211*, 118963. [[CrossRef](#)]
43. Kolasinski, P. Application of volumetric expanders in small vapour power plants used in distributed energy generation—Selected design and thermodynamic issues. *Energy Convers. Manag.* **2021**, *231*, 113859. [[CrossRef](#)]
44. Weiß, A.P. Volumetric expander versus turbine—which is the better choice for small ORC plants. In Proceedings of the 3rd ASME ORC conference, Brussels, Belgium, 12–14 October 2015; pp. 1–10.
45. Capata, R.; Pantano, F. Expander design procedures and selection criterion for small rated organic rankine cycle systems. *Energy Sci. Eng.* **2020**, *8*, 3380–3414. [[CrossRef](#)]
46. Pantano, F.; Capata, R. Expander selection for an on board ORC energy recovery system. *Energy* **2017**, *141*, 1084–1096. [[CrossRef](#)]

47. Kolasiński, P. The Influence of the Heat Source Temperature on the Multivane Expander Output Power in an Organic Rankine Cycle (ORC) System. *Energies* **2015**, *8*, 3351–3369. [[CrossRef](#)]
48. Petr, V.; Kolovratnik, M. Wet steam energy loss and related Baumann rule in low pressure steam turbines. *Proc. Inst. Mech. Eng. Part A J. Power Energy* **2013**, *228*, 206–215. [[CrossRef](#)]
49. Kolasiński, P.; Błasiak, P.; Rak, J. Experimental and Numerical Analyses on the Rotary Vane Expander Operating Conditions in a Micro Organic Rankine Cycle System. *Energies* **2016**, *9*, 606. [[CrossRef](#)]
50. Kolasiński, P. Application of the Multi-Vane Expanders in ORC Systems—A Review on the Experimental and Modeling Research Activities. *Energies* **2019**, *12*, 2975. [[CrossRef](#)]